

Subband and transport calculations in double n -type δ -doped quantum wells in Si

I. Rodriguez-Vargas, and L. M. Gaggero-Sager

Citation: [Journal of Applied Physics](#) **99**, 033702 (2006); doi: 10.1063/1.2168024

View online: <https://doi.org/10.1063/1.2168024>

View Table of Contents: <http://aip.scitation.org/toc/jap/99/3>

Published by the [American Institute of Physics](#)

Articles you may be interested in

[Weak localization thickness measurements of Si:P delta-layers](#)

[Applied Physics Letters](#) **85**, 6362 (2004); 10.1063/1.1842366

[Angle-dependent bandgap engineering in gated graphene superlattices](#)

[AIP Advances](#) **6**, 035309 (2016); 10.1063/1.4944495

[Encapsulation of phosphorus dopants in silicon for the fabrication of a quantum computer](#)

[Applied Physics Letters](#) **81**, 3197 (2002); 10.1063/1.1516859

[Investigating the regrowth surface of Si:P \$\delta\$ -layers toward vertically stacked three dimensional devices](#)

[Applied Physics Letters](#) **95**, 233111 (2009); 10.1063/1.3269924

[Impact of Si growth rate on coherent electron transport in Si:P delta-doped devices](#)

[Applied Physics Letters](#) **95**, 142104 (2009); 10.1063/1.3245313

[Enhancing electron transport in Si:P delta-doped devices by rapid thermal anneal](#)

[Applied Physics Letters](#) **93**, 142105 (2008); 10.1063/1.2996582

AIP | Journal of Applied Physics SPECIAL TOPICS



Subband and transport calculations in double n -type δ -doped quantum wells in Si

I. Rodriguez-Vargas^{a)} and L. M. Gaggero-Sager

Facultad de Ciencias, Universidad Autónoma del Estado de Morelos, Avenida Universidad 1001, Colonia Chamilpa, 62210 Cuernavaca, Morelos, México

(Received 28 June 2005; accepted 22 December 2005; published online 2 February 2006)

The Thomas-Fermi approximation is implemented in two coupled n -type δ -doped quantum wells in Si. An analytical expression for the Hartree-Fock potential is obtained in order to compute the subband level structure. The longitudinal and transverse levels are obtained as a function of the impurity density and the interlayer distance. The exchange-correlation effects are analyzed from an impurity density of 8×10^{12} to $6.5 \times 10^{13} \text{ cm}^{-2}$. The transport calculations are based on a formula for the mobility, which allows us to discern the optimum distance between wells for maximum mobility. © 2006 American Institute of Physics. [DOI: 10.1063/1.2168024]

I. INTRODUCTION

Recently, an improvement in the incorporation of different dopants such as Ge, P, Er, As, Sn, N, and O in Si has become possible.^{1–14} The n -type δ -doped quantum wells in Si provide an ideal system not only for investigating the physics at extremely high carrier densities but also for potential technological applications.^{15–17}

Single and multiple δ -doped structures have been reported experimentally^{18–24} and theoretical.^{25–32} Theoretical and experimental studies of the energy-level structure in n -type δ -doped layers in Si have been performed by resonant tunneling experiments and self-consistent calculations.^{18–20} Besides, the electrical activities and the carrier mobilities have been investigated by Hall measurements.²¹ Self-consistent calculations have been performed in single and multiple δ -doped Si structures.²⁵ The electronic structure as a function of the doping concentration (n_{2D}) and the periods (d) has been analyzed. The influence of n_{2D} and d on the subband energies and occupancies, potential profiles, Fermi-level position, and miniband widths is reported.

Double δ -doped quantum wells have attracted attention since the proposal by Zheng *et al.*,³³ due to the improvement in the transport properties. Theoretical and experimental works in which the properties of double δ -doped QWs are analyzed have been reported in the literature.^{33–46} These studies have been performed in GaAs,^{33–41} Si,^{42–45} and ZnSe.⁴⁶ In n -type double δ -doped quantum wells in Si there are two representative works.^{42,44} The electrical transport between locally grown δ -doped layers spaced 63–146 nm has been investigated.⁴² Current-voltage measurements show symmetrical diode characteristics for a donor density of $2 \times 10^{13} \text{ cm}^{-2}$. Transport measurements in two closely Sb δ -doped layers with a donor density of $2 \times 10^{13} \text{ cm}^{-2}$ and a distance between wells of $l=120 \text{ \AA}$ have been performed.⁴⁴ It is found that the room-temperature mobility is enhanced by a factor of 2 compared with the corresponding single δ -doped well or the homogeneous-doped layers. This mobility enhancement is attractive to optimized electronic devices.

In this work we present the results obtained for the electronic levels and the relative mobility as a function of the doping density and the distance between δ wells by means of the Thomas-Fermi (TF) approximation and a phenomenological formula for the mobility previously proposed and applied to p -type δ -doped systems.^{40,45,46} We also paid attention to the exchange-correlation effects, comparing the Hartree and Hartree-Fock calculations.

II. THEORETICAL APPROXIMATION

We consider n -type double δ -doped layers perpendicular to the growth direction ([001]) of a Si host crystal. The ionized donors and two-dimensional electron gas (2DEG) form a V-shaped potential. We will describe this potential using the local-density Thomas-Fermi approximation.

The ideal-gas relations are supposing valid at each point, that is, the electron density can be written as

$$n(\mathbf{r}) = \frac{1}{3\pi^2} \frac{p_F^3(\mathbf{r})}{\hbar^3}, \quad (1)$$

where p_F is the Fermi radius in the momentum space. The probability of finding an electron between p and $p+dp$ is

$$I_r(\mathbf{p})d\mathbf{p} = \frac{4\pi p^2 dp}{4/3\pi p_F^3} \theta(p_F - p). \quad (2)$$

The kinetic energy of a single electron can be written as

$$t = \frac{1}{2m^*} \int_0^{p_F} p^2 I_r(\mathbf{p})d\mathbf{p} = \frac{3}{2m^* p_F} \int_0^{p_F} p^4 dp, \quad (3)$$

integrating the former equation and using the relation between $n(z)$ and $p_F(z)$ Eq. (1) is possible to write the energy functional of the kinetic energy as

$$T = \int n(\mathbf{r})t(\mathbf{r})d\mathbf{r} = \frac{3}{10m^*} \int n(z)[3\pi^2\hbar^3 n(z)]^{2/3} dz, \quad (4)$$

where $m^* = (m_l^2 m_t)^{1/3}$ is the geometric average, with m_l and m_t the longitudinal and transverse electron effective masses. The energy functional corresponding to the interaction be-

^{a)}Electronic mail: irv@buzon.uaem.mx

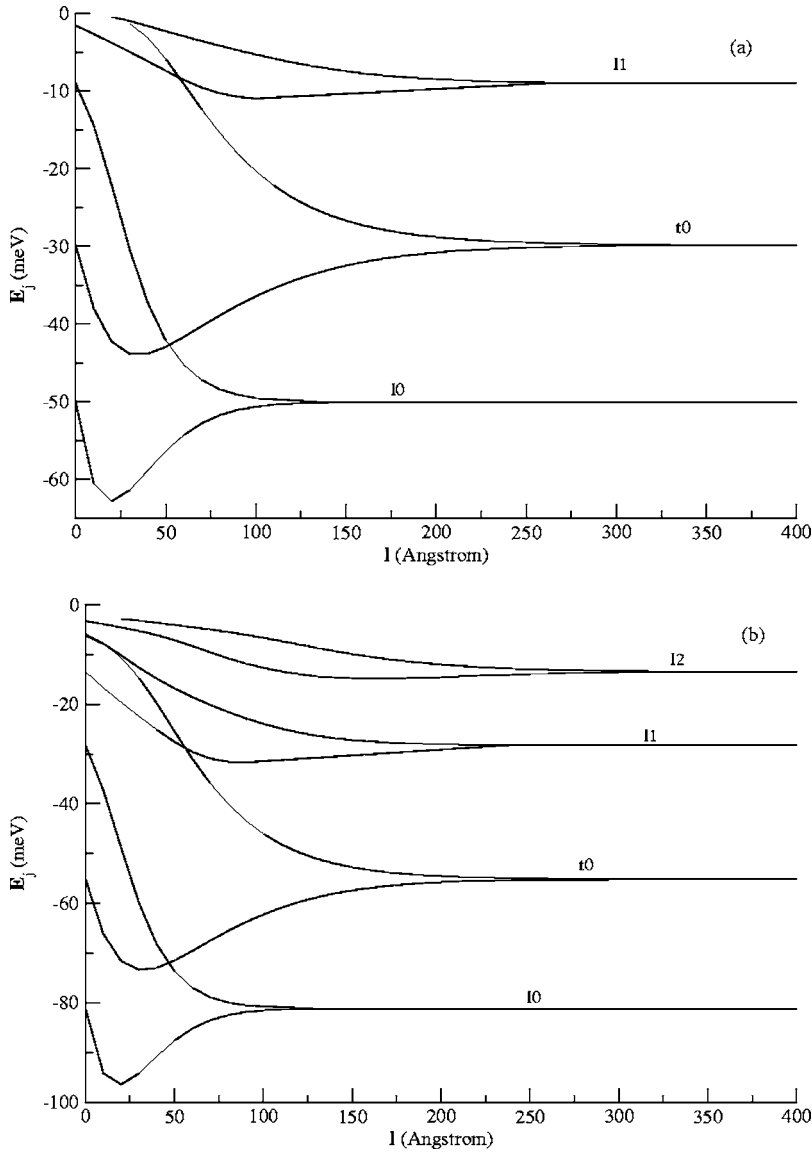


FIG. 1. Longitudinal and transverse electron levels vs the distance between wells, omitting (a) and considering (b) the exchange-correlation effects. The impurity density n_{2D} is $8 \times 10^{12} \text{ cm}^{-2}$.

tween the carrier cloud and each plane of ionized impurities is

$$V_{ei} = \int n(r)V_i(r)dr = \frac{2\pi e^2 n_{2D}}{\epsilon_r} \int n(z)(|z+l/2| + |z-l/2|)dz, \quad (5)$$

where $V_i(r)$, n_{2D} , ϵ_r , and l are the potential of the impurity planes, the two-dimensional impurity density, the relative dielectric constant, and the distance between δ wells, respectively. The energy functional associated to the electron-electron interaction comes as⁴⁷

$$V_{ee} = -\frac{\pi e^2}{\epsilon_r} \iint n(z)n(z')|z-z'|dzdz'. \quad (6)$$

Constructing the Thomas-Fermi energy density functional and taking the variation through standard procedures we can arrived to the classical Thomas-Fermi equation⁴⁷

$$n(z) = \frac{(2m^*)^{3/2}}{3\pi^2 \hbar^3} [\mu - V_H(z)]^{3/2}, \quad (7)$$

with μ and $V_H(z)$ representing the chemical and the Hartree potential, respectively.

The exchange and correlation effects are taking into account within the framework of the local-density approximation (LDA), therefore the exchange and correlation potential can be written as

$$V_{xc}(z) = -\left[1 + \frac{0.7734r_s}{21} \ln\left(1 + \frac{21}{r_s}\right)\right] \left(\frac{2}{\pi\alpha r_s}\right) R_y^*, \quad (8)$$

where

$$r_s = [4\pi a_0^* n(z)/3]^{-1/3}. \quad (9)$$

In these expressions $a_0^* = \epsilon_r \hbar^2 / (m^* e^2)$ is the effective Bohr radius, $R_y^* = e^2 / (2\epsilon_r a_0^*)$ is the effective Rydberg constant, and $\alpha = [4/(9\pi)]^{1/3}$.

Substituting the relation between the carrier density and the Hartree potential in the former equation for r_s , and r_s in (8), the exchange and correlation potential can be written in terms of the Hartree one

$$V_{xc}^*(z) = -c \left(1 + a \frac{\ln\{1 + b[\mu^* - V_H^*(z)]^{1/2}\}}{[\mu^* - V_H^*(z)]^{1/2}} \right) \times [\mu^* - V_H^*(z)]^{1/2}, \quad (10)$$

the latter equation is given in a.u. $V_{xc}^* = V_{xc}/R_y^*$, $V_H^* = V_H/R_y^*$, and $\mu^* = \mu/R_y^*$. $a = 0.7734/21[4/(9\pi)]^{-1/3}$, $b = 21[4/(9\pi)]^{1/3}$, and $c = 2/\pi$. The self-consistent Hartree potential of the double δ -doped quantum wells is⁴⁸

$$V_H^*(z) = \mu^* - \frac{\beta^2}{(\beta|z + l/2| + z_0)^4}, \quad (11)$$

where $\beta = 2/(15\pi)$ and $z_0 = (\beta^3/\pi n_{2D}^{a.u.})^{1/5}$. Finally substituting (11) in (10), the total potential $V^*(z) = V_H^*(z) + V_{xc}^*(z)$ is

$$V^*(z) = - \frac{\beta^2}{(\beta|z + l/2| + z_0)^4} - c \left\{ \frac{\beta}{(\beta|z + l/2| + z_0)^2} + a \ln \left[1 + \frac{b\beta}{(\beta|z + l/2| + z_0)^2} \right] \right\}. \quad (12)$$

The latter equation summarized the proposed model for the exchange-correlation (Hartree-Fock) calculations. Instead of carrying out numerically troublesome self-consistent calculations, we simply solve a Schrödinger-like effective-mass equation, thus obtaining the corresponding ladder of the elec-

tron levels. When we omit the exchange-correlation term, we are referring to the Hartree calculations.

The conduction-band edge of Si consists of six equivalent valleys located close to the six equivalent X points of the Brillouin-zone boundary. The effective masses are anisotropic for each valley and it is possible to separate Schrödinger-like equations for each valley. Since the Schrödinger-like equations are the same for valleys of the same type, the eigenvalues are also identical. Thereby, the longitudinal eigenvalues will be twofold degenerate, and the transverse fourfold. The motion in the directions of x and y is plane wave. Then the corresponding electron density is

$$n(z) = \sum_{nj} N_n^j |F_n^j(z)|^2. \quad (13)$$

Here the index j runs over all six valleys. Assuming zero temperature, N_n^j is

$$N_n^j = \frac{m_{\parallel j}^*}{\pi \hbar^2} (E_F - E_{nj}) \Theta(E_F - E_{nj}), \quad (14)$$

where $m_{\parallel j}^* = m_t$ if $j = z, \bar{z}$ and $m_{\parallel j}^* = (m_x m_y)^{1/2}$ if $j = x, \bar{x}, y, \bar{y}$. E_F represents the Fermi energy and Θ the Heaviside step function.

Besides, this method allows us to study the transport properties of the system. We only consider the ionized acceptor scattering mechanism because it is the most important at low temperature. The Coulomb scattering potential due to ionized impurities is considered as distributed randomly in the doped layer. We take the ratio of the mobility of double δ -doped (DDD) to single δ -doped (SDD) QWs.

$$\mu_{rel}^{\delta} = \frac{\mu_{DDD}}{\mu_{SDD}} = \frac{\sum_j m_{\parallel j}^* \sum_i \int |F_e^{\delta}(z')|^2 (k_F^{\delta} - E_i^{\delta}) |z'| dz'}{\sum_j m_{\parallel j}^* \sum_i \int |F_e^{2\delta}(z')|^2 (k_F^{2\delta} - E_i^{2\delta}) (|z' - l/2| + |z' + l/2|) dz'}, \quad (15)$$

where $F_e^{\delta}(z')$, k_F^{δ} , and E_i^{δ} [$F_e^{2\delta}(z')$, $k_F^{2\delta}$, and $E_i^{2\delta}$] are the envelope function, the Fermi level, and the i th level, respectively, of the SDD (of the DDD). Equation (15) is valid for $T=0$ K.

The influence of the temperature onto the electronic structure has been calculated self-consistently.⁴⁹ The results

have shown a slight modification of the level structure when the temperature is less than 6 meV (77 K). In such a case the electronic structure can be taken as that corresponding to 0 K and the thermal effect can be considered as a charge redistribution. Then, the mobility expression would be (as dependent on temperature)

$$\mu_{rel}^{\delta} = \frac{\sum_j m_{\parallel j}^* \sum_i \int |F_e^{\delta}(z')|^2 \ln[1 + e^{(k_F^{\delta} - E_i^{\delta})/k_B T}] |z'| dz'}{\sum_j m_{\parallel j}^* \sum_i \int |F_e^{2\delta}(z')|^2 \ln[1 + e^{(k_F^{2\delta} - E_i^{2\delta})/k_B T}] (|z' - l/2| + |z' + l/2|) dz'}. \quad (16)$$

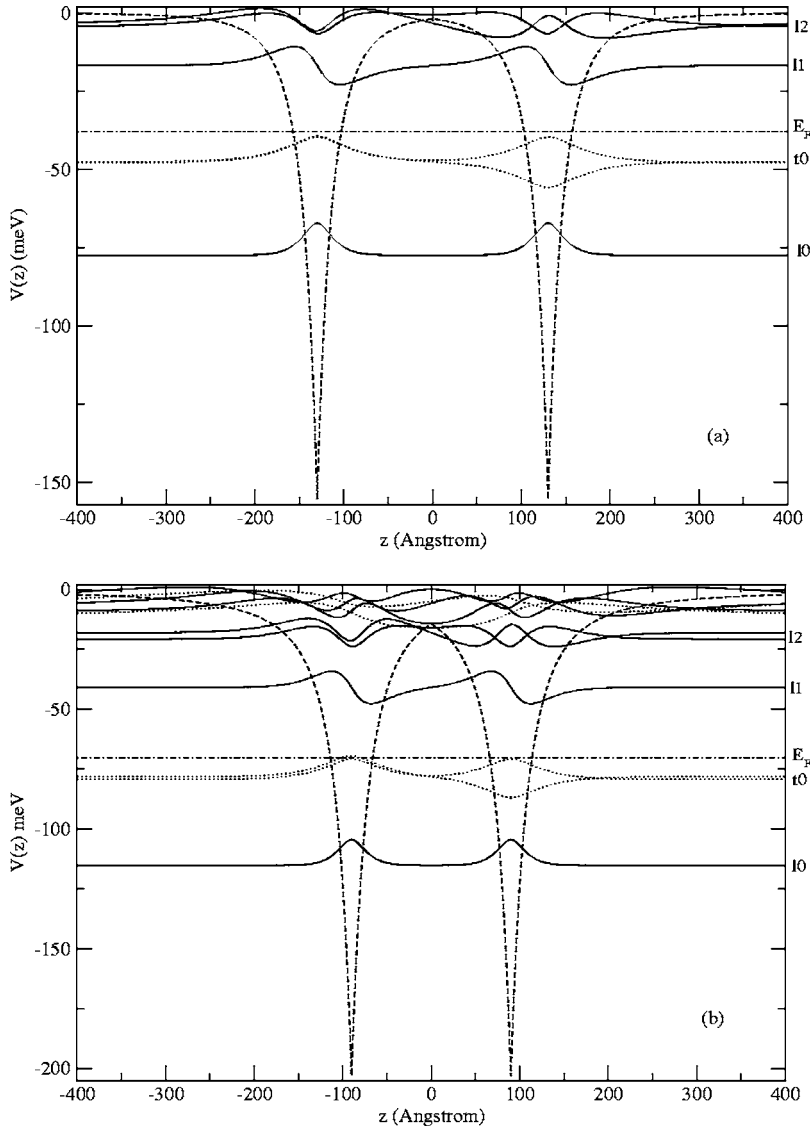


FIG. 2. Potential profile, Fermi energy, and longitudinal and transverse electron wave functions for a donor density $n_{2D} = 1.3 \times 10^{13} \text{ cm}^{-2}$ and interlayer distances $l = 260 \text{ \AA}$ (a) and 180 \AA (b). The solid and dashed lines represent the longitudinal and transverse electron wave functions, while the dashed-dot line represents the Fermi level, omitting (a) and considering (b) exchange-correlation effects.

It is worth mentioning that the former phenomenological formulas have been applied successfully to p -type δ -doped systems.^{40,46}

III. RESULTS AND DISCUSSION

The starting parameters for n -type δ -doped quantum wells in Si are $m_l^* = 0.9163$, $m_t^* = 0.1905$, and $\epsilon_r = 12.1$. The doping concentration is varied from 8.0×10^{12} to $3.0 \times 10^{14} \text{ cm}^{-2}$. This interval for n_{2D} includes its experimentally interesting values.

The electron energy levels as a function of the interwell distance are presented in Fig. 1 for a donor density $n_{2D} = 8 \times 10^{12} \text{ cm}^{-2}$. Figures 1(a) and 1(b) correspond to the calculations omitting and taking into account the exchange-correlation effects. The trends are similar for both calculations. As we can see from Fig. 1 the longitudinal basic level (the transverse ground level) becomes degenerate for distances around 140 and 120 Å (300 and 250 Å), omitting and considering exchange-correlation effects. For the transverse ground level a difference of around 50 Å is found, comparing both calculations. A similar thing happens for the other levels, depending on the concentration and on which level is

observed. As the donor density increases the degeneration takes place a lesser distance between wells as well as the difference in the degeneration distance with and without exchange-correlation effects for the different levels is reduced. In the high density limit ($6.5 \times 10^{13} \text{ cm}^{-2}$) differences were not found concerning to the degeneration distance for both calculations. Therefore, the exchange-correlation effects are significant when the donor density is lower.

In Fig. 2 we present the potential profile and the eigenfunctions, normalized to 1, for a donor density $n_{2D} = 1.3 \times 10^{13} \text{ cm}^{-2}$ and distances between impurity planes $l = 260 \text{ \AA}$ (a) and $l = 180 \text{ \AA}$ (b). The solid lines correspond to the longitudinal electron levels, while the dashed lines to the transverse ones. When the exchange-correlation potential is considered in the calculations, Fig. 2(b), the potential depth is 203.3 meV, while omitting these effects a value of 155.5 meV is obtained, Fig. 2(a).

Self-consistent potential calculations were performed in Sb δ -doped Si quantum well with a surface barrier height $e\Phi = 0.7 \text{ eV}$, an ionic charge of $1.3 \times 10^{13} \text{ cm}^{-2}$ spread over 1 nm, and a background doping of $2 \times 10^{16} \text{ cm}^{-3}$.¹⁸ A small forward bias eV_g of 0.035 was considered. The energy levels

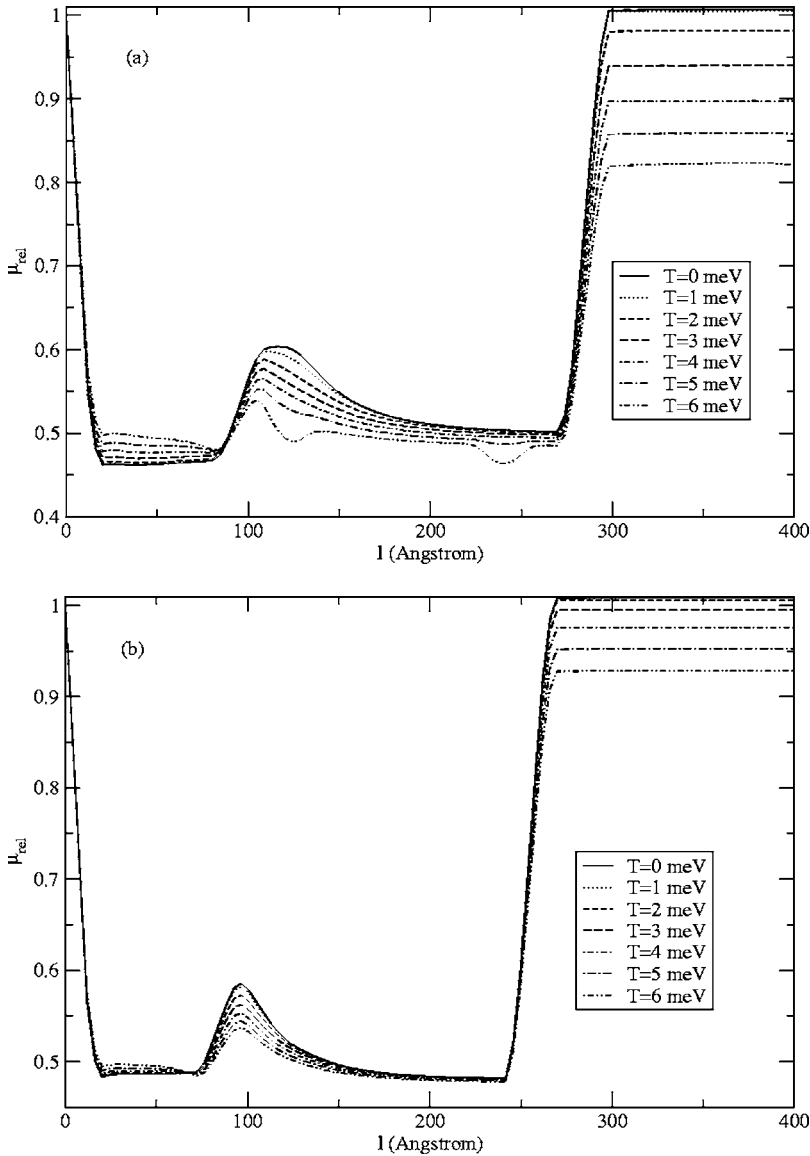


FIG. 3. Relative mobility vs the distance between δ wells for an impurity density of $8 \times 10^{12} \text{ cm}^{-2}$ (a) and $1.3 \times 10^{13} \text{ cm}^{-2}$ (b). The different curves represent different temperatures in the range of 0–77 K. The exchange-correlation effects are considered in the calculations.

obtained are $E_{l_0} = -55.0 \text{ meV}$, $E_{t_0} = -1.9 \text{ meV}$, $E_{l_1} = 37.1 \text{ meV}$, and $E_{l_2} = 64.7 \text{ meV}$ all with respect to the Fermi level, $E_F \approx -70.8 \pm 4.4 \text{ meV}$. Here, the Fermi energy is measured with respect to the conduction-band edge. Theoretical calculations were carried out in order to obtain the subband level structure.¹⁹ Solving the Poisson equation an analytical expression for the confining potential was obtained. It was allowed a small but finite width of the δ -doping layer, homogeneous doping in the layer, and homogeneous unintentional background doping. Then, the energy levels were determined by means of the WKB integral by iteration procedure.¹⁹ The calculation was performed for a sample with δ -doping density $n_{2D} = 1.3 \times 10^{13} \text{ cm}^{-2}$, a background doping level of $5.0 \times 10^{15} \text{ cm}^{-2}$, and a Schottky-barrier height $\Phi = 0.75 \text{ eV}$. The energies of -35 and -8 meV are obtained for the longitudinal and transverse ground levels. The energy reference is the Fermi energy in the well. Our calculations ($l=0$) give $E_{l_0} = -44.8 \text{ meV}$, $E_{t_0} = -8.4 \text{ meV}$, $E_{l_1} = 29.3 \text{ meV}$, and $E_{l_2} = 50.9 \text{ meV}$ measured with respect to Fermi energy, $E_F = -70.3 \text{ meV}$. The Fermi level is measured with respect to the conduction-band edge.

The quantum levels were determined through tunneling spectroscopy for an impurity density of $1.3 \times 10^{13} \text{ cm}^{-2}$.¹⁸ The dI/dV_g tunneling characteristic showed evidence at positive V_g for the occupied longitudinal ground level at $\sim -55 \text{ meV}$. The same situation with the same experimental techniques¹⁹ showed that the basic longitudinal level has an energy of -35 meV . Indeed, in these systems the experimental error is 10 meV . Therefore, the ground level for an impurity density of $1.3 \times 10^{13} \text{ cm}^{-2}$ using tunneling spectroscopy experiments is $-45 \pm 10 \text{ meV}$. Our calculations ($l=0$) give $E_{l_0} = -44.8 \text{ meV}$ measured with respect to E_F .

In Figs. 3(a) and 3(b) we present the dependence of the mobility versus the distance between wells, for two donor densities of 8×10^{12} and $1.3 \times 10^{13} \text{ cm}^{-2}$, respectively. For $l=0$ and $l \geq 300 \text{ \AA}$ the energy-level structure corresponds to a single δ doped, therefore the mobility ratio must tend to unity. These two limiting cases are well fulfilled as we can see from Figs. 3(a) and 3(b). A main peak for the mobility is found around 120 and 100 \AA at $T=0 \text{ K}$ for the two aforementioned concentrations, respectively. Varying the kinetic energy from 0 to 6 meV by an amount of 1 meV , the main

TABLE I. Energy levels (E_{l0} and E_{l0}), Fermi energy (E_F), and the potential depth (V_0) obtained by means of the Hartree (H) and exchange-correlation (XC) potential calculations for n -type DDD QWs in Si as a function of the impurity density n_{2D} , and with $l=0$ Å. All energies in the table are measured with respect to the conduction-band edge.

n_{2D} (10^{12} cm $^{-2}$)	E_{l0} (H) (meV)	E_{l0} (XC) (meV)	E_{l0} (H) (meV)	E_{l0} (XC) (meV)	E_F (H) (meV)	E_F (XC) (meV)	V_0 (H) (meV)	V_0 (XC) (meV)
8	-50.1	-81.2	-29.8	-55.2	-24.3	-50.6	-105.5	-145.3
13	-77.5	-115.2	-47.6	-78.2	-38.0	-70.3	-155.5	-203.3
65	-321.7	-394.2	-217.3	-279.3	-160.8	-224.8	-563.6	-651.4

peak in Fig. 3(a) is shifted to around 100 Å, while in Fig. 3(b) remains at the same distance. These peaks have a direct connection with the degeneration distance of the longitudinal basic level, due to the special rearrangement of the electron charge in the superior electron energy levels. Since, when the degeneration occurs an increase in the charge density of the superior levels is presented. This increase is small indeed but significant for the mobility because on one hand, the transverse levels have a small effective mass, and on the other, the excited levels have nodes in the impurity planes, for which the electronic charge is located in the undoped region of DDD QW, thereby the dispersion rate goes down, and consequently the mobility increases.

Finally, in Table I we present (for $l=0$) the paramount features of the n -type DDD QWs in Si for three different impurity densities, 8×10^{12} , 1.3×10^{13} , and 6.5×10^{13} cm $^{-2}$, omitting (H) and considering exchange-correlation effects (XC). As we can see from the mentioned table, the Fermi energy, the potential depth, and the longitudinal and the transverse electron levels have important changes when the exchange-correlation effects are considered. These changes have more relevance as the impurity density is increased.

IV. CONCLUSIONS

In summary, the subband levels and the relative mobility in double n -type δ -doped quantum wells are presented. The Thomas-Fermi approximation is implemented in order to obtain an analytical expression for the Hartree-Fock potential. The system is analyzed as a function of the donor density as well as the distance between the δ wells. This expression is important for possible device applications as well as for more elaborated self-consistent calculations. It is shown in this work that the Thomas-Fermi approximation, a simple model that keeps a great amount of physics, works remarkably well.

¹T. Fuse, K. Kawamoto, T. Shiizaki, E. Tazou, M. Katayama, and K. Oura, Jpn. J. Appl. Phys., Part 1 **37**, 2625 (1998).

²C. Sheng, F. Lin, D. Gong, J. Wan, Y. Fan, and X. Wang, Jpn. J. Appl. Phys., Part 1 **37**, 1206 (1998).

³J. Wan, Z. M. Jiang, D. W. Gong, Y. L. Fan, C. Sheng, X. Wang, Q. J. Jia, W. L. Zheng, and X. M. Jiang, Phys. Rev. B **59**, 10697 (1999).

⁴T. Kobayashi, C. F. MacConville, G. Derenbos, M. Iwaki, and M. Aono, Appl. Phys. Lett. **74**, 673 (1999).

⁵S. Agan, O. A. Mironov, E. H. C. Parker, and T. E. Whall, Semicond. Sci. Technol. **15**, 551 (2000).

⁶J. Yuhara, K. Morita, J. Falta, B. H. Muller, and M. Horn-von Hoegen, Surf. Interface Anal. **31**, 754 (2001).

⁷O. D. Dubon, P. G. Evans, J. F. Chervinsky, M. J. Aziz, F. Spaepen, J. A. Golovchenko, M. F. Chisholm, and D. A. Muller, Appl. Phys. Lett. **78**, 1505 (2001).

⁸L. Oberbeck, N. J. Curson, M. Y. Simmons, R. Brenner, A. R. Hamilton, S. R. Schofield, and R. G. Clark, Appl. Phys. Lett. **81**, 3197 (2002).

⁹P. Leveque, J. S. Christensen, A. Y. Kuznetsov, B. G. Svensson, and A. N. Larsen, J. Appl. Phys. **91**, 4073 (2002).

¹⁰V. K. Paliwal, A. G. Vedeshwar, and S. M. Shivaprasad, Surf. Sci. Lett. **513**, L397 (2002).

¹¹A. Fujimoto, K. Kobori, T. Ohyama, and S. Ishida, Phys. Status Solidi B **230**, 273 (2002).

¹²Y. Jeong, M. Sakuraba, and J. Murota, Appl. Surf. Sci. **224**, 197 (2004).

¹³L. Oberbeck, N. J. Curson, T. Hallam, M. Y. Simmons, G. Bilger, and R. G. Clark, Appl. Phys. Lett. **85**, 1359 (2004).

¹⁴K. E. J. Goh, L. Oberbeck, and M. Y. Simmons, Phys. Status Solidi A **202**, 1002 (2005).

¹⁵X. Zhu, X. Zheng, M. Pak, M. O. Tanner, and K. L. Wang, Thin Solid Films **321**, 201 (1998).

¹⁶P. E. Thompson, K. D. Hobart, M. E. Twigg, S. L. Rommel, N. Jin, P. R. Berger, R. Lake, A. C. Seabaugh, P. H. Chi, and D. S. Simons, Thin Solid Films **380**, 145 (2000).

¹⁷C. Rivas, R. Lake, W. R. Frensley, G. Klimeck, P. E. Thompson, K. D. Hobart, S. L. Rommel, and P. R. Berger, J. Appl. Phys. **94**, 5005 (2003).

¹⁸H. P. Zeindl, T. Wegehaupt, I. Eisele, H. Oppolzer, H. Reisinger, G. Tempel, and F. Koch, Appl. Phys. Lett. **50**, 1164 (1987).

¹⁹H.-M. Li, K.-F. Berggren, W.-X. Ni, B. E. Sernelius, M. Willander, and G. V. Hansson, J. Appl. Phys. **67**, 1962 (1990).

²⁰I. Eisele, Superlattices Microstruct. **6**, 123 (1989).

²¹H.-J. Gossmann and F. C. Unterwald, Phys. Rev. B **47**, 12 618 (1993).

²²B. Sciana, D. Radziejewicz, B. Paszkiewicz, M. Tlaczala, P. Sitarek, R. Kudrawiec, J. Misiewicz, J. Kovac and Florovic, Vacuum **74**, 263 (2004).

²³S. Modesti, R. Duca, P. Finetti, G. Ceballos, M. Piccin, S. Rubini, and A. Franciosi, Phys. Rev. Lett. **92**, 086104 (2004).

²⁴T. Kurosawa, T. Komatsu, M. Sakuraba, and J. Murota, Mater. Sci. Semicond. Process. **8**, 125 (2005).

²⁵L. M. R. Scolfaro, D. Beliaev, R. Enderlein, and J. R. Leite, Phys. Rev. B **50**, 8699 (1994).

²⁶E. Ozturk, Y. Ergun, H. Sari, and I. Sokmen, J. Appl. Phys. **91**, 2118 (2002).

²⁷E. Ozturk and I. Sokmen, J. Phys. D **36**, 2457 (2003).

²⁸J. Osvald, Physica E (Amsterdam) **23**, 147 (2004).

²⁹J. Osvald, J. Phys. D **37**, 2655 (2004).

³⁰E. Ozturk, H. Sari, Y. Ergun, and I. Sokmen, Appl. Phys. A: Mater. Sci. Process. **80**, 167 (2005).

³¹V. A. Vettchinkina, A. Blom, and K. A. Chao, Phys. Rev. B **72**, 045303 (2005).

³²G. Qian, Y.-C. Chang, and J. R. Tucker, Phys. Rev. B **71**, 045309 (2005).

³³X. Zheng, T. K. Carns, K. L. Wang, and B. Wu, Appl. Phys. Lett. **62**, 504 (1993).

³⁴P. M. Koenraad, A. C. L. Heessels, F. A. P. Blom, J. A. A. J. Perenboom, and J. H. Wolter, Physica B **184**, 221 (1993).

³⁵H. M. Shieh, W. C. Hsu, and C. L. Wu, Appl. Phys. Lett. **63**, 509 (1993).

³⁶C. L. Wu, W. C. Hsu, H. M. Shieh, and W. C. Liu, Appl. Phys. Lett. **64**, 3027 (1994).

³⁷H.-M. Sheih, C.-L. Wu, W.-C. Hsu, Y.-H. Wu, and M.-J. Kao, Jpn. J. Appl. Phys., Part 1 **33**, 1778 (1994).

³⁸G.-Q. Hai, N. Studart, and F. M. Peeters, Phys. Rev. B **52**, 11273 (1995).

³⁹E. Ozturk, Y. Ergun, H. Sari, and I. Sokmen, Appl. Phys. A: Mater. Sci. Process. **77**, 427 (2003).

⁴⁰I. Rodriguez-Vargas, L. M. Gaggero-Sager, and V. R. Velasco, Surf. Sci. **537**, 75 (2003).

⁴¹E. Ozturk and I. Sokmen, Superlattices Microstruct. **35**, 95 (2004).

⁴²W. Kiunke, E. Hammerl, I. Eisele, D. Schulze, and G. Gobsch, J. Appl. Phys. **72**, 3602 (1992).

- ⁴³T. K. Carns, X. Zheng, and K. L. Wang, *Appl. Phys. Lett.* **62**, 3455 (1993).
- ⁴⁴H. H. Radamson, M. R. Sardela, Jr., O. Nur, M. Willander, B. E. Sernelius, W.-X. Ni, and G. V. Hansson, *Appl. Phys. Lett.* **64**, 1842 (1994).
- ⁴⁵I. Rodriguez-Vargas and L. M. Gaggero-Sager, *Phys. Status Solidi C* **2**, 3634 (2005).
- ⁴⁶I. Rodriguez-Vargas, L. M. Gaggero-Sager, and J. C. Martinez-Orozco, *Phys. Status Solidi B* **242**, 1043 (2005).
- ⁴⁷L. M. Gaggero-Sager, *Modell. Simul. Mater. Sci. Eng.* **9**, 1 (2001).
- ⁴⁸L. Ioriatti, *Phys. Rev. B* **41**, 8340 (1990).
- ⁴⁹L. M. Gaggero-Sager and R. Pérez-Alvarez, *Appl. Phys. Lett.* **70**, 212 (1997).